International Journal of Computational and Experimental Science and Engineering (IJCESEN)

Vol.10-No:4 (2024) pp. 630-638
http://www.ijcesen.com

ISSN: 2149-9144

Research Article

Characterization of Microstructure of Fe-TiC and Fe-B_4C Composites Using Ultrasonic Measurements

Vildan ÖZKAN BİLİCİ[1]*, Ahmet YÖNETKEN[2]

[1]Afyon Kocatepe University, Science and Arts Faculty, Physics Department, 03200, Afyonkarahisar -Turkey
* **Corresponding Author Email:** vildanozkan@aku.edu.tr - **ORCID:** 0000-0002-3077-2103

[2]Afyon Kocatepe University, Technology Faculty, Mechatronics Engineering Dept., 03200, Afyonkarahisar, Turkey
Email: yonetken@aku.edu.tr - **ORCID:** 0000-0003-1844-7233

Article Info:

DOI: 10.22399/ijcesen.434
Received : 28 August 2024
Accepted : 08 October 2024

Keywords

Ultrasonic Velocity
Hardness
Porosity
Composite
Pulse-Echo Method

Abstract:

In this paper, an iron (Fe) matrix reinforced with boron carbide (B_4C) and titanium carbide (TiC) was produced by conventional furnace sintering at the same compositions and temperatures. Experimental data on the change in ultrasonic velocity parameter, densities and porosity of these two different microstructure composites during microstructure development are reported. The microstructural phases were characterized by metallographic studies and hardness measurements. The velocities of ultrasonic longitudinal waves were measured by the pulse- echo method using the transmit/receive probe. In the Fe-TiC composite sample, ultrasound longitudinal wave velocity, hardness and porosity increased linearly depending on the increasing amount of TiC. In the Fe-B_4C composite sample, on the other hand, there is a linear increase in general depending on the increasing amount of B_4C, and there is a sharp decrease in the amount of 8.33% B_4C. The reason for this decrease and other results are explained by taking into account SEM and XRD analyzes.

1. Introduction

Composite materials are new materials made of two or more component materials with significantly different physical or chemical properties and have different properties when combined. Cermets are also materials consisting of heterogeneous combinations of metals and alloys with one or more ceramic phases. Composites generally get their strength from hard and brittle reinforcement materials. Matrix materials provide toughness and ductility to the composite. Mechanical and physical properties are not only dependent on the matrix structure but also directly related to the type, size and distribution of carbides in the structure [1-5]. In addition, some alloying elements such as silicon, titanium and boron segregate to the matrix/carbide interface and contribute to the development of mechanical properties by modifying eutectic carbides [6-7]. In order to improve the mechanical properties and strength of these materials, alloying processes can be carried out with alloying elements such as carbide-forming vanadium, tungsten, titanium, boron and niobium [8-11].

The development and use of new wear-resistant lightweight composites based on boron carbide due to their excellent properties such as low density, high wear resistance, elastic modulus and hardness, and titanium carbide due to its desired properties such as high hardness, high melting temperature, high modulus and good wettability and thermodynamic stability in molten Fe has many areas of use including metallurgy, armor applications, hardening of metal surfaces, cutting tools and abrasives, hydrogen production and storage, glass industry, aerospace and chemical industry [12-21].

In this study, experimental data on the changes in ultrasonic velocity parameters, densities, hardness and porosity during microstructure development of Fe-TiC and Fe-B_4C composites are reported. Microstructural phases are characterized by metallographic studies and hardness measurements. For this purpose, microstructure examinations and hardness measurements were applied to materials with different titanium carbide and boron carbide ratios in the pressed and heat-treated position and the results obtained were comparatively examined.

2. Material and Methods

2.1 Fe-TiC and Fe-B_4C composite preparation

The properties of the metallic and ceramic powders used in this study are Fe powders from Sigma Aldrich with 99.8% purity and particle size less than 70 μm, B_4C powders with 99.9% purity and particle size less than 100 μm, TiC powders with 99.5% purity and 10μm particle size were used. $98.33\%\mathrm{Fe}\begin{cases}1.66\%\mathrm{TiC}\\1.66\%B_4C\end{cases}$, $96.66\%\mathrm{Fe}\begin{cases}3.33\%\mathrm{TiC}\\3.33\%B_4C\end{cases}$, $95\%\mathrm{Fe}\begin{cases}5\%\mathrm{TiC}\\5\%B_4C\end{cases}$, $93.33\%\mathrm{Fe}\begin{cases}6.66\%\mathrm{TiC}\\6.66\%B_4C\end{cases}$, $91.66\%\mathrm{Fe}\begin{cases}8.33\%\mathrm{TiC}\\8.33\%B_4C\end{cases}$ samples were obtained by powder metallurgy method. The powders were weighed with precision scales and mixed in a mixer for 24 hours to ensure that the composition was homogeneous. Fe, TiC and B4C powders were pressed in a cylindrical high-strength steel mold with a diameter of 15 mm and a length of about 5 mm using a uniaxial cold hydraulic press under a pressure of 300 kg/cm^2. The raw densities of the pressed Fe-TiC and Fe-B_4C composite samples were measured and then sintered at 1200°C in an Argon gas atmosphere for 2 hours in a conventional tube furnace. After the sintering process, the samples were left to cool naturally under the argon atmosphere in the oven. The hardness of Fe-TiC and Fe-B_4C composite samples was measured with METTEST-HT (Vickers) brand hardness tester. In order to make microstructural and metallographic evaluations, SEM and EDX analyzes were performed with a LEO 1430 VP scanning electron microscope equipped with an Oxford EDX analyzer.

2.2 Ultrasonic pulse-echo method

The purpose of using the ultrasonic method is to determine the properties of the material under investigation due to the deviations observed in the ultrasonic response occurring in an ideal environment and to understand the wave-material interaction. The ultrasonic method is the most preferred NDT technique for finding defects such as microstructure and physical properties, errors, cracks and fractures by performing material characterization without damaging the tested part.

The experimental data set obtained in the study includes raw data collected by the ultrasonic pulse-echo method on Fe-TiC and Fe-B_4C composite samples. The surfaces of the measured objects were carefully scanned point by point. Pulse-echo measurement of the stimulated sound pulse is performed at each of these measurement points. The time signal resulting from a pulse-echo measurement is often called an A-scan in ultrasonic testing [22]. Such an A-scan is based on the logic that it maps the sound pressure of the received signal in amplitude to a certain flight time of the pulse.

The schematic diagram showing the ultrasonic experimental setup is presented in Figure 1. In the study, Sonatest Sitescan 150s brand flaw detector, which is a fully functional device and thickness gauge that includes many productivity-enhancing features for ultrasonic measurement, was used in pulse echo measurement for ultrasonic testing.

The ultrasonic flaw detector works on the principle of measuring the flight time of high-frequency sound across the test piece, as well as evaluating the amplitude of reflected or transmitted echoes. It has two test modes: pulse echo and transmit/receive.

A single-cycle sinusoidal signal was generated by a function generator (Sonatest Technologies, Inc.) to drive the transmitter. The excitation voltage of the input signal was set at 10 V to provide a reliable signal with sufficient energy for subsequent analysis. A contact transducer (Sonatest SLH4-10) with a diameter of 10 mm and a nominal center frequency of 4 MHz was used during the experiment.

In the pulse-echo experiment (Figure 1(a)), the ultrasonic wave propagating through the sample was reflected by the bottom interface and then received by the same transducer. To improve the signal-to-noise ratio, measurements were taken 5 times from the sample surface and averaged. To ensure good contact between the transducer and sample and to allow smooth probe movement during testing

Sonatest sonagel-W liquid gel was used as a coupling fluid between the probes and the sample. The speed of the waves through the thickness of the samples was determined by Equation (1).

$$V_L = \frac{2\times d}{t} \qquad (1)$$

where d: thickness of the composite sample (mm), t: time of flight between adjacent back wall signals (μs) and V: velocity of the ultrasonic longitudinal wave (m/s) [23-24]. At the same time, a calibration check was made after the test to minimize errors. The data received is raw data recorded point by point on a measurement grid defined on two surfaces of the sample.

3. Results and Discussions

Composite samples produced by sintering at 1200°C with powder metallurgy technique; interpreted in terms of hardness, density, microstructure, porosity, SEM and XRD.

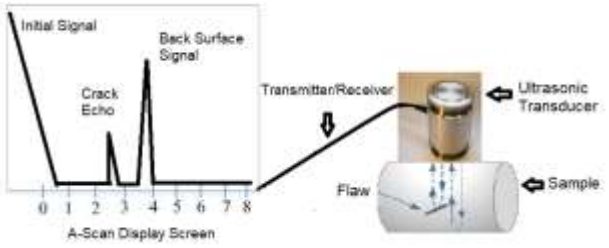

(a)

(b)

Figure 1. *Schematic diagram of a) A scan plot b) the ultrasonic testing (UT) set-up*

SEM analysis results of Fe/TiC and Fe/B_4C composite samples prepared with TiC and B_4C powders taken at different volume ratios sintered at 1200 °C are shown in Figure 2 and Figure 3. Also, the XRD analysis results of Fe-TiC and Fe-B_4C composite samples sintered at the temperature of 1200°C were shown in Figure 4 for two hours. As can be understood from the XRD analysis results, the presence of TiC and B_4C peaks in the pattern indicates that the Fe, metallic phase is reinforced with TiC and B_4C carbide phases. As can be seen, Fe, TiC and B_4C phases are formed in the produced composite. The measured ultrasonic longitudinal wave velocities, density, Vickers hardness and porosity values of TiC/Fe samples and B_4C/Fe samples in this study are summarized in Table 1 and Table 2, respectively.

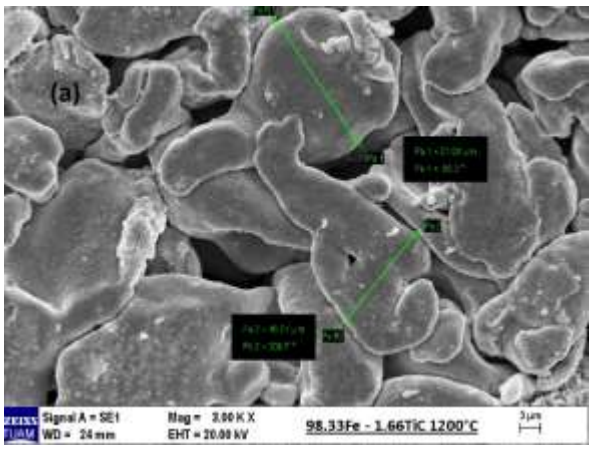

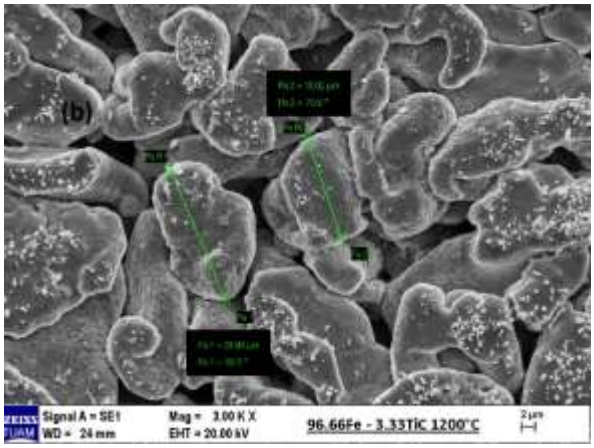

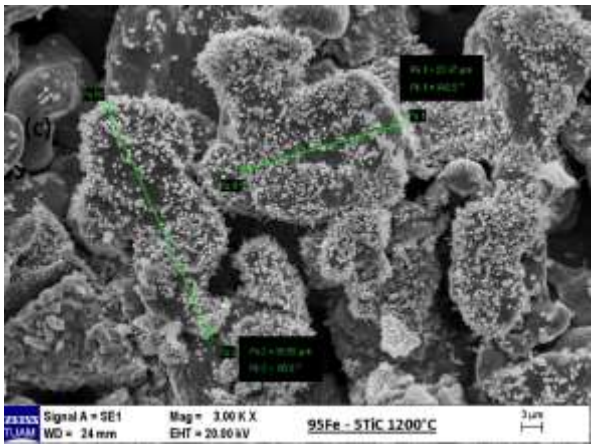

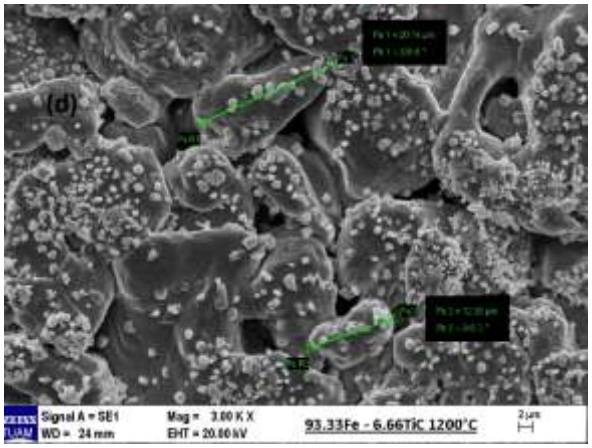

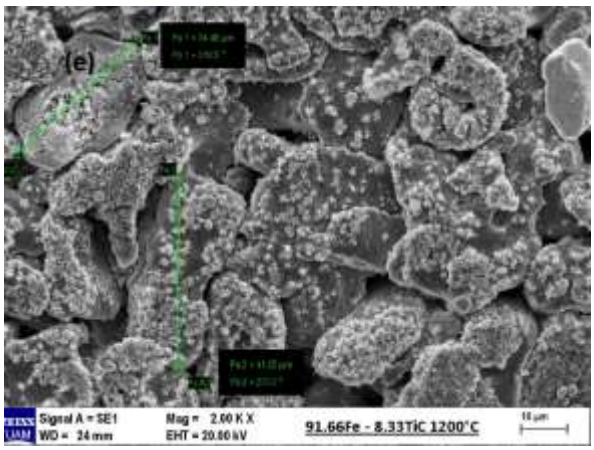

Figure 2. *SEM images of Fe/TiC composite samples.*

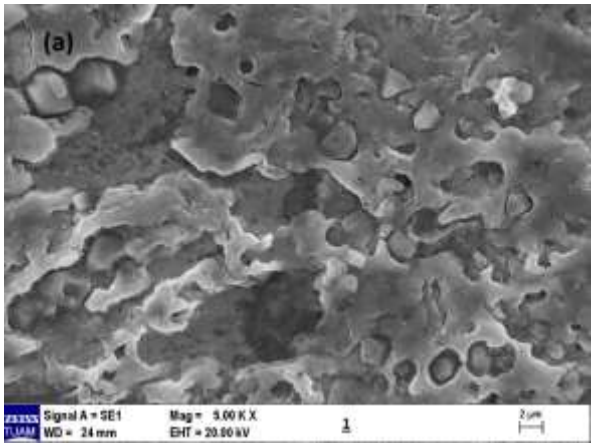

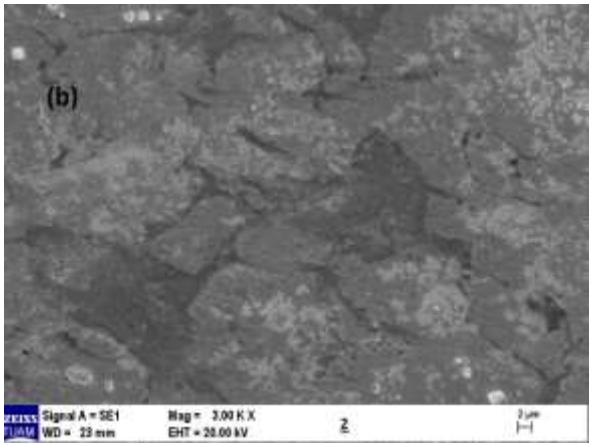

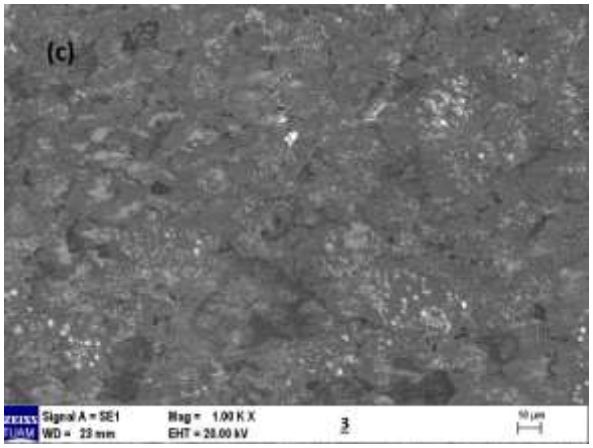

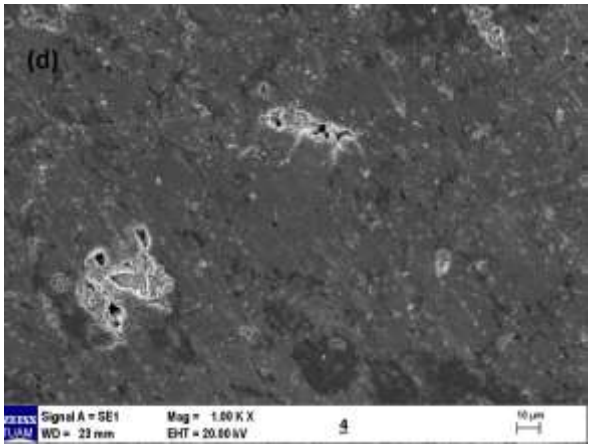

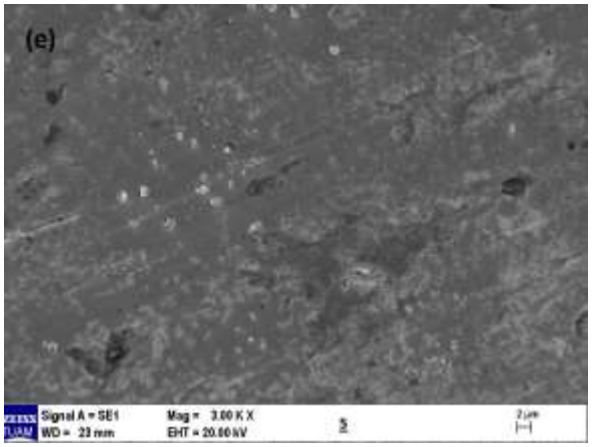

Figure 3. *SEM images of Fe/B_4C composite samples.*

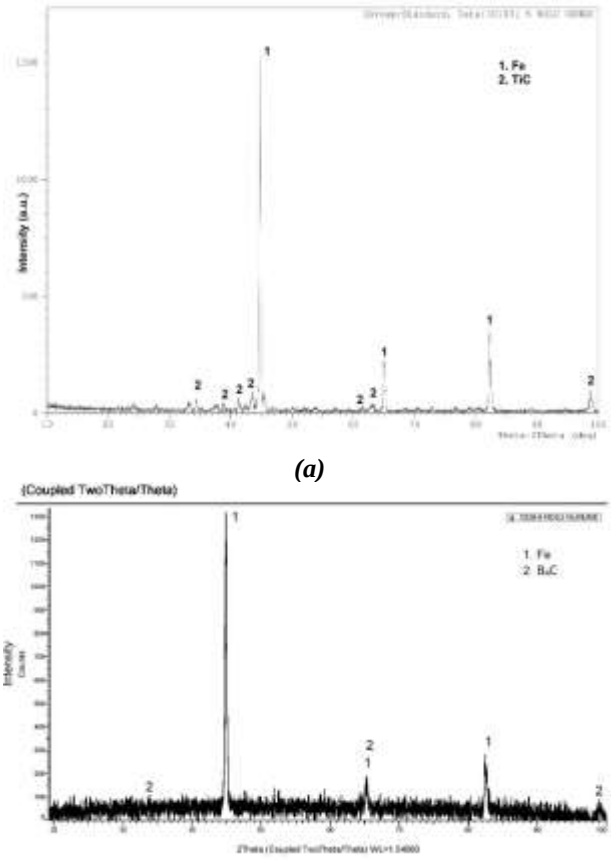

(a)

(b)

Figure 4. *The XRD analysis results of Fe-TiC and Fe-B_4C composite samples.*

Table 1. *Physical and mechanical properties for the TiC/Fe composites as a function of TiC content.*

Composite Samples	V_L (m/s)	Hardness (HV)	Density (g/cm^3)	Porosity (%)
98.33%Fe-1.66%TiC	3275±0.5%	140.6	8.56	40.1
96.66%Fe-3.33%TiC	3556±0.5%	137.1	7.72	34.5
95%Fe-5%TiC	3752±0.6%	122.4	7.49	32.8
93.33%Fe-6.66%TiC	3867±0.3%	107.5	7.35	31.9
91.66%Fe-8.33%TiC	3925±0.2%	103.6	7.22	27.5

Table 2. *Physical and mechanical properties for the B_4C/Fe composites as a function of B_4C content.*

Composite Samples	V_L (m/s)	Hardness (HV)	Density (g/cm^3)	Porosity (%)
98.33%Fe-1.66%B_4C	3333±0.6%	48.3	7.78	37.7
96.66%Fe-3.33% B_4C	3476±0.5%	60.7	7.56	35.3
95%Fe-5% B_4C	3647±0.6%	66.18	7.23	35.2
93.33%Fe-6.66% B_4C	3921±0.5%	72.65	6.80	32.8
91.66%Fe-8.33% B_4C	4096±0.6%	79.63	6.29	29.9

3.1 Hardness Measurement Results

Hardness testing is performed to determine the suitability of a material for a particular application or specific process to which the material is subjected and to determine the internal structural strength of that material. Hardness measurements always indicate characteristics of the properties of both binder and carbide phases; these can be significantly affected by factors such as crystal structure, shape and size of carbide grains, chemical, physical and mechanical properties of the sintered carbide/metal interface, and residual stresses between phases [25-27]. Hardness measurements were made using the METTEST-HT (Vickers) microhardness tester. Micro hardness measurements were measured at a feed rate of 0.5 mm/min by averaging the hardness values taken from 10 different points for each sample. Hardness measurement results in Vickers units are given in Figure 5. The change in hardness values is clearly seen by adding different amounts of Fe, TiC and B_4C elements, and as the percentage values of titanium carbide and boron carbide compound increased, the hardness values decreased and increased respectively. The hardness of TiC/Fe composites followed a decreasing trend with the further increase of TiC content. It can be seen that the increase in TiC addition leads to a decrease in hardness for TiC/Fe composites of 1.66%, 3.33%, 5%, 6.66% and 8.33% by volume. When measuring the Vickers hardness of composites, it is important to consider some characteristics of the materials used. Composites obtained with some carbides tend to be hard and relatively brittle materials, so some of the energy delivered is consumed in creating cracks. Therefore, at high loads, the energy will be dissipated by the formation of cracks and the measured overall hardness value will decrease. While the porosity value of TiC/Fe composite was 8.33% by volume (27.5%), it weakened the bearing capacity of TiC hard grains. It can be concluded that the hardness of the composites depends on the collective effect of TiC content and porosity. Composites containing 1.66% TiC by volume reached the highest hardness of 140.6 Vickers. It can be seen that the increase in B_4C addition leads to an increase in hardness for B_4C/Fe composites of 1.66%, 3.33%, 5%, 6.66% and 8.33% by volume. Boron carbide, used in the military, industry and industry, is a substance with excellent structural hardness, low density, large cross-sectional surface area for neutron absorption and high chemical stability. The hardness of Fe-B_4C composite samples increases with decreasing initial porosity and increasing iron doping. Therefore, the increase in the hardness of the composite is due to the uniform distribution of the reinforcement. Composites containing 8.33% B_4C by volume reached the highest hardness of 79.63 Vickers.

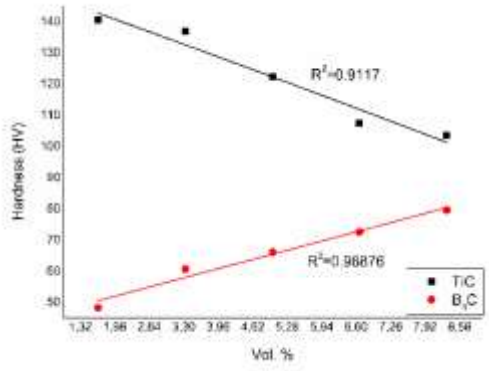

Figure 5. *Variation plot of Vickers hardness against different volume percentages of TiC/Fe and B_4C/Fe samples*

3.2 Porosity and Density Measurement Results

Porosity is expressed as the volumetric ratio of pores in the material. The density and porosity of TiC/Fe and B_4C/Fe composite samples were measured by the Archimedes method. In the study, porosity was measured as the ratio of the porosity, that is, the void volume of the composite material, to the total volume of the composite material. This porosity amount was shown in table values as percentage (%). As seen in the SEM images, it is seen that there are voids on the surface or internal structures of the composite material and the density decreases. Both porosity values and density values decreased due to increasing volume percentages of TiC/Fe and B_4C/Fe composite samples heat treated at the same sintering temperature. Porosity is closely related to the density of the material and the general nature of the compounds of the elements and the presence of voids between these compounds. Additionally, reducing the grain size in the internal structure of the material may make it difficult for iron powders to penetrate the preform, which may further contribute

to the decrease in relative density. Figure 6 shows the microstructure of prepared TiC/Fe and B_4C/Fe composite samples with varying porosity values against different volume percentages.

The densities of the samples obtained after sintering ($d = m/V$) were calculated using the calculation formula (Figure 7). Here m is the mass of the sintered sample; V is the volume of the sintered sample calculated geometrically. When Figure 7 is examined, the highest density is in 1.66% TiC added mixture as 8.56 g/cm^3 and 1.66% B_4C added mixture as 7.78 g/cm^3, respectively, and the lowest density is 7.22 g/cm^3 in the mixture with 8.33%TiC additive and 6.29 g/cm^3 in the mixture with 8.33% B_4C additive, respectively. According to these values, density and porosity change in direct proportion.

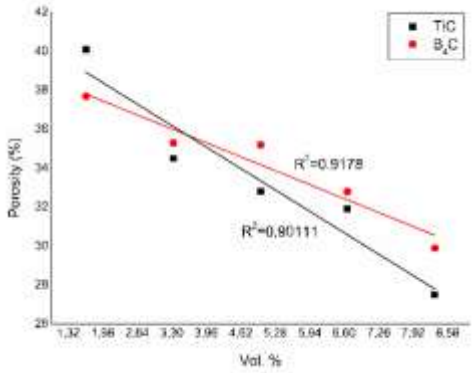

Figure 6. *Graph of porosity variation against different volume percentages of TiC/Fe and B_4C/Fe samples*

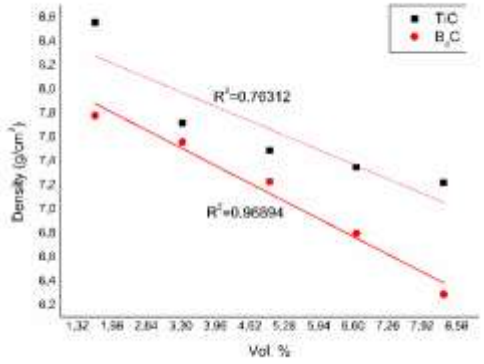

Figure 7. *Relationship between percent volume values and relative density of TiC/Fe and B_4C/Fe composite samples.*

3.3 Ultrasonic Wave Velocity Measurement Results

Ultrasonic pulse velocity (UPV) is also determined by the vibration and rotational energy of intermolecular interactions within the microstructure. Ultrasonic vibration waves in boron carbide and titanium carbide reinforced composites into iron powders are mainly related to absorption in molecules and scattering of particles. The wave propagates faster in a continuous solid; that is, a higher porosity level tends to reduce the ultrasonic pulse velocity. Considering the porosity results of the composites, it decreases depending on the behaviour of UPV.

Ultrasonic pulse velocity data for Fe/TiC composite samples range from 3275 m/s to 3925 m/s, while ultrasonic pulse velocity data for B_4C/Fe composite specimens range from 3333 m/s to 4096 m/s.

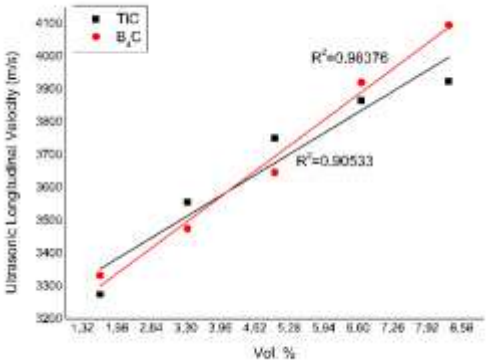

Figure 8. *Relationship between percentage volume values and ultrasonic longitudinal wave velocity values of TiC and B_4C composite samples.*

Figure 8 shows the graphs of the interaction effect of varying TiC and B_4C percentage values on the ultrasonic pulse velocity of both TiC/Fe and B_4C/Fe composites. B_4C has a higher R^2 value of 0.98376 in the chart, revealing that it offers good statistical predictability for the data. The percentage contribution shown in Table 1 and Table 2 reveals that UPV is affected by the volume fraction factor. UPV increases as the proportion of TiC and B_4C in the matrix increases, as shown in Figure 8, which also leads to a decrease in the porosity level. We can state that the increase in pores contributes to the delay in wave propagation. Thus, a higher matrix phase content also reduces the void volume, increasing the dispersion of ultrasonic pulse waves. There are also other works done on related subject and reported imported results [28-38].

4. Conclusions

This article describes the effect of the particle system in the composite structure formed by TiC and B_4C reinforcements on iron powders with different volume percentages on the ultrasonic pulse velocity, mechanical and physical responses. In particular, correlation analyses of hardness, density, porosity and UPV are performed against TiC and B_4C reinforcements taken at different volume percentages. The surface and distribution of the evaluated particles first affect their physical properties and then their mechanical properties.

While hardness values decrease with increasing TiC reinforcement percentage in the Fe-TiC composite sample, they increase with increasing B_4C reinforcement percentage in the Fe-B_4C composite sample. Fe-TiC carbide compounds were found to be brittle and hard materials. From the results obtained, it was determined that carbide materials were hard and considering their hardness values, they were listed as B_4C > TiC. According to SEM and XRD analyses, the density and porosity values of the supported composite samples decrease as the amount of reinforcement increases. Ultrasonic pulse velocity increases with increasing percentage rates; because it did not prevent the advancement of ultrasonic waves due to the fact that the pore sizes in the structure were very small and gradually decreased. In general, physical and mechanical responses are mainly affected by the surface area and distribution of particles.

Author Statements:

- **Ethical approval:** The conducted research is not related to either human or animal use.
- **Conflict of interest:** The authors declare that they have no known competing financial interests or personal relationships that could have appeared to influence the work reported in this paper
- **Acknowledgement:** The authors declare that they have nobody or no-company to acknowledge.
- **Author contributions:** The authors declare that they have equal right on this paper.
- **Funding information:** The authors declare that there is no funding to be acknowledged.
- **Data availability statement:** The data that support the findings of this study are available on request from the corresponding author. The data are not publicly available due to privacy or ethical restrictions.

References

[1] Fan, Q., Duan, H., Xing, X. (2024). A review of composite materials for enhancing support, flexibility and strength in exercise. *Alex. Eng. J.* 94:90-103. https://doi.org/10.1016/j.aej.2024.03.048

[2] Nettersheim, I. H. M. S., Guevara Sotelo, N. S., Verdank, J. c., Masania, K. (2024). Engineered living composite materials. *Compos. Sci. Technol.* 256:110758. https://doi.org/10.1016/j.compscitech.2024.110758

[3] Lu, G., Yu, T., (2013). 11- Composite materials and structures. *Energy Absorption of Structures and Materials/Woodhead Publishing Series in Metals and Surface Engineering*, 317-350. https://doi.org/10.1533/9781855738584.317

[4] Cheng, Z.-Q., Liu, H., Tan, W., (2024). Advanced computational modelling of composite materials. *Eng. Fract. Mech.* 305:110120. https://doi.org/10.1016/j.engfracmech.2024.110120

[5] Veidt, M., Liew, C. K., (2013). 17 - Non-destructive evaluation (NDE) of aerospace composites: structural health monitoring of aerospace structures using guided wave ultrasonics. *Non-Destructive Evaluation (NDE) of Polymer Matrix Composites/Woodhead Publishing Series in Composites Science and Engineering*. 449-479. https://doi.org/10.1533/9780857093554.3.449

[6] Koç, F. G., Çöl, M., (2018). The Effect of Titanium on Microstructure and Hardness in High Alloy White Cast Iron. *Düzce University Journal of Science and Technology -DUBITED*. 6:669-675.

[7] Han, L., Liu, L., Chen, T., Qian, Z., Li, J., Zuo, C., Gan, G., (2024). Preparation of three-dimensional boron nitride-aluminum oxide dual thermal network resin-based composite materials and their performance study. *Polymer*. 308:127382. https://doi.org/10.1016/j.polymer.2024.127382

[8] Saurah, A., Meghana, C. M., Singh, P. K., Verma, P. C., (2022). Titanium-based materials: synthesis, properties, and applications., *Mater. Today*. 56:1:412-419. https://doi.org/10.1016/j.matpr.2022.01.268

[9] Lyon, S. B., (2010). 3.15 - Corrosion of Tantalum and Niobium and their Alloys. *Reference Module in Materials Science and Materials Engineering/ Shreir's Corrosion.* 3:2135-2150. https://doi.org/10.1016/B978-044452787-5.00102-5

[10] Günen, A., Kurt, B., Milner, P., Gök, M. S., (2019). Properties and tribological performance of ceramic-base chromium and vanadium carbide composite coatings. *Int. J. Refract. Met. Hard Mater.* 81:333-344. https://doi.org/10.1016/j.ijrmhm.2019.03.019

[11] Yönetken, A. B., Yönetken A., (2024). Characterization of electroless Ni(ZrO2) coated Ti alloy fabricated by sintering for biomedical materials. *J. Ceram. Process. Res.* 25:97-103. https:// doi.org/ 10.36410/jcpr.2024.25.1.97

[12] Benic, L. S., Subic, J., Erman, Z., (2020). Effect of boron and tungsten carbides on the properties of tic-reinforced tool steel matrix composite produced by powder metallurgy. *Arch. Metall. Mater.* 65(2):539-547. https://doi.org/10.24425/amm.2020.132791

[13] Kommel, L., Kimmari, E., (2006). Boron Carbide Based Composites Manufacturing and Recycling Features. *Mater. Sci. (Medžiagotyra).* 12(1):48-52. ISSN 1392–1320.

[14] Frage, N., Hayun, S., Kalabukhov, S., Dariel, M. P., (2007). The effect of Fe addition on the densification of B4C powder by spark plasma sintering. *Powder Metall. Met. Ceram.* 46:533–538. https://doi.org/10.1007/s11106-007-0082-9

[15] Baglyuk, G.A., Napara-Volgina, S.G., Vol'fman, V.I., Mamonova, A. A., Pyatachuk, S. G., (2009). Thermal synthesis of Fe–B4C powder master alloys. *Powder Metall. Met. Ceram.* 48:381–383. https://doi.org/10.1007/s11106-009-9156-1

[16] Pascu, C. I., Gheorghe, Ş., Rotaru, A., Nicolicescu, C., Ciotera, N., Rosca, A. S., Sarbu, D., Rotaru, P., (2020). Ti-based composite materials with enhanced

thermal and mechanical properties. *Ceram. Int.* 46(18), Part B: 29358-29372. https://doi.org/10.1016/j.ceramint.2020.08.207

[17] Hamamcı, M., Nair, F., Cerit, A. A., (2016). Investigation of the metallographic and mechanical properties of FE/B4C-B composites produced at different sintering temperatures, *International Conference on Material Science and Technology in Cappadocia (IMSTEC'16).* 158-163.

[18] Sigl, L. S., Processing and mechanical properties of boron carbide sintered with TiC. *J. Eur. Ceram. Soc.* 18(11):1521-1529. https://doi.org/10.1016/S0955-2219(98)00071-5

[19] Rajabi, A., Ghazali, M. J., Daud, A. R., (2015). Effect of second phase morphology on wear resistance of Fe-TiC composites *J. Tribol.* 4: 1-9.

[20] Xiang, S., Ren, S., Liang, Y., Zhang, X. (2019). Fabrication of titanium carbide-reinforced iron matrix composites using electropulsing-assisted flash sintering. *Mater. Sci. Eng. A.* 768:138459. https://doi.org/10.1016/j.msea.2019.138459

[21] Xiao, M., Zhang, Y., Wu, Y., Qiu, Z., Zhou, C., Zhuo, S., Liu, M., Zeng, D., (2021). Preparation, mechanical properties and enhanced wear resistance of TiC-Fe composite cermet coating. *Int. J. Refract. Met. Hard Mater.* 101:105672. https://doi.org/10.1016/j.ijrmhm.2021.105672.

[22] Maack, S., Küttenbaum, S., Bühling, B., Borchardt-Giers, K., Aßmann, N., Niederleithinger, E. (2023). Low frequency ultrasonic pulse-echo datasets for object detection and thickness measurement in concrete specimens as testing tasks in civil engineering. *Data Brief.* 48:109233. https://doi.org/10.1016/j.dib.2023.109233

[23] Toozandehjani, M., Ostovan, F., Shamshirsaz, M., Matori, K.A., Shafiei, E. (2021). Velocity and attenuation of ultrasonic wave in Al–Al_2O_3 nanocomposite and their correlation to microstructural evolution during synthesizing procedure. *J. Mater. Res. Technol*. 15:2529-2542. https://doi.org/10.1016/j.jmrt.2021.09.065

[24] Sahu, S., Bhope, K., Prajapati, A., Mehta, M., Tailor, H., Bhattacharyay, R., Khirwadkar, S.S. (2022). Sonic velocity measurement in molten Pb–Li (16) at high temperature for ultrasonic flowmeter applications. *Flow Meas. Instrum.* 88:102271. https://doi.org/10.1016/j.flowmeasinst.2022.102271

[25] Shatov, A. V., Panomarev, S. S., Firstov, S. A., (2014). 1.09 - Hardness and Deformation of Hardmetals at Room Temperature. *Reference Module in Materials Science and Materials Engineering Comprehensive Hard Materials.* 1:267-299. https://doi.org/10.1016/B978-0-08-096527-7.00009-X

[26] Yönetken, A., Bilici Özkan, V., (2022). Ultrasonic and Mechanical Characterization of Borided Ceramic–Metal Composite. *Russ. J. Nondestruct. Test.* 58(9):779-789. https://doi.org/10.1134/S1061830922090091

[27] Hering, B., Gestrich, t., Steinborn, C., Vornberger, A., Pötschke, J., (2023). Influence of Alternative Hard and Binder Phase Compositions in Hardmetals on Thermophysical and Mechanical Properties. *Metals.* 13(11):1803. https://doi.org/10.3390/met13111803

[28] EVCİN, A., GÜNEY, H., & BEZİR, N. (2021). Sol-gel Preparation of Silan based Titania Hybrid Composite Thin Film. *International Journal of Computational and Experimental Science and Engineering*, 7(1), 25–28. Retrieved from https://www.ijcesen.com/index.php/ijcesen/article/view/142

[29] Basmaci, A. N., & Filiz, S. (2024). Investigation of Electromagnetic Wave Propagation in Triple Walled Carbon Nanotubes . *International Journal of Computational and Experimental Science and Engineering*, 10(1);27-32. https://doi.org/10.22399/ijcesen.241

[30] AYAZ, A., OZDEMİR, G. D., ERCAN, U. K., SEVER, K., & KORKUT, N. (2024). An experimental study of effect of atmospheric plasma treatment on shear strength of adhesively bonded GFRP-aluminum joints. *International Journal of Computational and Experimental Science and Engineering*, 10(2);160-167. https://doi.org/10.22399/ijcesen.316

[31] KUTU, N. (2024). Neutron Shielding Properties of Cellulose Acetate CdO-ZnO Polymer Composites. *International Journal of Computational and Experimental Science and Engineering*, 10(2);203-206. https://doi.org/10.22399/ijcesen.322

[32] BIYIK, S. (2024). Influence of Polyethylene Glycol and Methanol Additions on the Properties of Ball-Milled Cu4B4C Composite Powders. *International Journal of Computational and Experimental Science and Engineering*, 10(3);299-307. https://doi.org/10.22399/ijcesen.317

[33] ORUNCAK, B. (2023). Computation of Neutron Coefficients for B2O3 reinforced Composite. *International Journal of Computational and Experimental Science and Engineering*, 9(2), 50–53. Retrieved from https://www.ijcesen.com/index.php/ijcesen/article/view/189

[34] KARTAL, İlyas, & TUNÇ, M. (2024). Investigation of Mechanical Properties of Oak Sawdust Filled Polyester Composites . *International Journal of Computational and Experimental Science and Engineering*, 10(3);282-287. https://doi.org/10.22399/ijcesen.245

[35] KARTAL, İlyas, KASAP, K., & DEMİRER, H. (2023). Investigation of Mechanical Properties of Domestic Black Tea Waste Filled Vinylester Composites. *International Journal of Computational and Experimental Science and Engineering*, 9(4), 435–440. Retrieved from https://www.ijcesen.com/index.php/ijcesen/article/view/290

[36] İlyas Kartal, & Hilal Selimoğlu. (2024). Usability of Pine Sawdust and Cotton Together as Filler in Recycled Polypropylene Composites. *International Journal of Computational and Experimental Science and Engineering*, 10(2);174-180. https://doi.org/10.22399/ijcesen.244

[37] KARTAL, İlyas, & SELİMOĞLU, H. (2023). Investigation of the mechanical behavior of recycled

polypropylene-based composite materials filled with waste cotton and pine sawdust. *International Journal of Computational and Experimental Science and Engineering*, 9(4), 412–418. Retrieved from https://www.ijcesen.com/index.php/ijcesen/article/view/288

[38] DEMİREL, H., GÜNEŞ , A., & ŞAHİN, Ömer S. (2019). Recycling and Characterization of Metallic Chips Using Powder Metallurgy. *International Journal of Computational and Experimental Science and Engineering*, 5(3), 151–153. Retrieved from https://www.ijcesen.com/index.php/ijcesen/article/view/106